Applied Catalysis B: Environmental 100 (2010) 299–309

Contents lists available at ScienceDirect

Applied Catalysis B: Environmental

journal homepage: www.elsevier.com/locate/apcatb

Synthesis of biodiesel from the methanolysis of sunflower oil using PURAL® Mg–Al hydrotalcites as catalyst precursors

A. Navajas[a], I. Campo[a], G. Arzamendi[a], W.Y. Hernández[b], L.F. Bobadilla[b], M.A. Centeno[b], J.A. Odriozola[b], L.M. Gandía[a,*]

[a] Departamento de Química Aplicada, Edificio de los Acebos, Universidad Pública de Navarra, Campus de Arrosadía s/n, E-31006 Pamplona, Spain
[b] Instituto de Ciencia de Materiales de Sevilla, Centro Mixto CSIC-Universidad de Sevilla, Avda. Américo Vespucio 49, E-41092 Sevilla, Spain

ARTICLE INFO

Article history:
Received 24 May 2010
Received in revised form 30 July 2010
Accepted 5 August 2010
Available online 12 August 2010

Keywords:
Biodiesel
Hydrotalcite
Methanolysis
Sunflower oil
Transesterification

ABSTRACT

A series of commercial Mg–Al hydrotalcites have been used as catalyst precursors for the methanolysis of sunflower oil. The solids were characterized by low Mg/Al molar ratios in the 0.5–2.3 range. Additionally, a solid consisting mainly of $Mg(OH)_2$ but containing some Al (4.2 wt.%) was also employed. The as-received materials were inactive for biodiesel synthesis so calcination and rehydration in boiling water were considered as activation treatments. Among the calcined solids, only the material consisting of MgO was significantly active, achieving about 50% oil conversion after 24 h at 60 °C, methanol/oil molar ratio of 12 and 2 wt.% of catalyst. The effects of the calcination temperature in the 350–700 °C range have been investigated; calcination at 500 °C led to the best catalytic performance. In the case of the rehydrated materials, only the solids with the highest Mg/Al molar ratios recovered a well-ordered layered double hydroxide structure. These samples showed an improved catalytic activity compared with their calcined counterparts. A good correlation between catalytic activity and the basic properties determined using Hammett indicators and benzoic acid titration has been found. Rehydrated hydrotalcites were slightly more selective to biodiesel (75%) at intermediate levels of oil conversion than the calcined counterparts (66%). It has been verified that no Mg or Al leaching in the reaction mixture took place; however, the rehydrated samples deactivated significantly. In the case of MgO, after washing and calcination, the recycled catalyst gave 68% of the original oil conversion.

1. Introduction

There is a great interest in the development of renewable fuels due to growing concern on atmospheric pollution, global warming, and limited availability of traditional fossil fuels. In the European Union (EU), the recent Directive on the promotion of the use of energy from renewable sources has established general objectives to achieve a 20% share of energy from renewable sources in the EU's gross final consumption of energy and a 10% share of energy from renewable sources in each member state's transport energy consumption by 2020 [1]. One of the biofuels considered in this Directive is biodiesel, defined as methyl esters of diesel quality produced from vegetable or animal oil. Sustainability criteria are essential for the suitable development of biofuels [2–4]. For example, the EU's Directive states that the greenhouse gas emissions saving from the use of biofuels has to be at least 35% at present and 60% by 2018 [1,5].

Biofuels share by energy content in the EU's total road transport fuel consumption rose from 2.6% in 2007 to 3.4% in 2008, being the consumption of road fuel during this period 309 Mtoe. Biodiesel consumption increased from 5899 ktoe to 7900 ktoe between 2007 and 2008 equivalent to an increase of 33.9% [6]. Biodiesel is a mixture of esters obtained by the transesterification of triglycerides with methanol. This is a well-established industrial process that is carried out using homogeneous catalysts as NaOH, KOH or their methoxides that are readily dissolved in the alcohol [7–9]. However, heterogeneous catalysts would be preferable because they could be separated more easily, regenerated and reutilized. Moreover, operational problems linked to the hazardous, caustic and hygroscopic character of the homogeneous catalysts as well as wastewater generation and production costs would diminish [10–13]. In the recent years an increasing number of studies is being dedicated to the transesterification with methanol (methanolysis) of triglycerides using heterogeneous catalysts. Main issues with solid transesterification catalysts are low activity and, in many cases, lack of chemical stability in the reaction conditions. Among the solids reported it is worth mentioning several compounds of the alkaline-earth

* Corresponding author. Tel.: +34 948 169 605; fax: +34 948 169 606.
E-mail address: lgandia@unavarra.es (L.M. Gandía).

0926-3373/$ – see front matter © 2010 Elsevier B.V. All rights reserved.
doi:10.1016/j.apcatb.2010.08.006

metals, mainly of Ca and Mg [14–26], alumina- [27–33] and silica-supported [31,34–36] catalysts, phosphates [37–39], zeolites [40–43] and titanosilicates [41,44]. However, hydrotalcites are probably the materials that have gained most attention in the last few years as transesterification catalysts for biodiesel synthesis [12].

Hydrotalcite, or magnesium–aluminium hydroxycarbonate ($Mg_6Al_2(OH)_{16}CO_3{\cdot}4H_2O$), is a naturally occurring anionic clay that reversibly decomposes upon calcination forming a high-surface-area, mixed oxide with basic properties [45]. Hydrotalcite-like compounds are layered double hydroxides with general formula $[M_n^{2+}M_m^{3+}(OH)_{2(n+m)}]^{m+}[A^{x-}]_{m/x}{\cdot}yH_2O$, where M^{2+} and M^{3+} are divalent and trivalent metal cations, respectively, and A represents an anion (typically carbonate) that compensates the net positive charge of the brucite-like layers [46–48]. The anions and the water crystallization molecules are located in the interlayer space between two brucite-like sheets. These materials can be used as-synthesized or after different treatments as catalysts in a variety of organic reactions with potential applications for the production from large-scale basic to specialty chemicals [49].

The majority of the published works using hydrotalcites as catalysts or as precursors of transesterification catalysts for biodiesel synthesis have been performed with materials prepared at the laboratory. In this study, commercial hydrotalcites with different Mg/Al ratios have been considered for the methanolysis of sunflower oil with methanol. The effects of the calcination and rehydration processes on the catalytic performance of these solids have been investigated.

2. Experimental

2.1. Catalyst precursors and calcined and rehydrated samples

PURAL® MG hydrotalcites (*CONDEA/Sasol Germany GmbH, Inorganic Specialty Chemicals*) were employed as catalyst precursors. The following hydrotalcites were considered (their Mg/Al molar ratio is given between parentheses): PURAL® MG 30 (0.5), MG 50 (1.3), MG 61 (1.9) and MG 70 (2.3). Additionally, a sample consisting of $Mg(OH)_2$, PURAL® MG 100, was also included in this study. The as-received catalyst precursors will be referred to as HT_{30}-as, HT_{50}-as, HT_{61}-as, HT_{70}-as, and HT_{100}-as. According to the manufacturer specifications, these materials are aluminium magnesium hydroxy carbonate hydrates $Mg_{2x}Al_2(OH)_{4x+4}(CO_3){\cdot}nH_2O$ with x varying between 0.5 and 2.3. Carbonate content is about 10 wt.% and the maximum loss on ignition (3 h, 1000 °C) is in the 40–45% range. Due to its high Al content, HT_{30}-as contains a significant amount of boehmite (γ-AlO(OH)), whereas HT_{100}-as contains 4.2 wt.% Al.

The as-received materials were inactive for the transesterification with methanol of sunflower oil under typical reaction conditions. Two activation treatments have been considered in this work with the aim of developing catalytic activity. The first one was calcination for 6 h under static air at temperatures between 350 and 700 °C using a heating rate of 1.5 °C/min. The second activation treatment was rehydration. The solids were first calcined at 500 °C as described above. Then, they were allowed to cool in air and while being sufficiently hot they were transferred to a vacuum desiccator and allowed to reach room temperature. Finally, the solids were rehydrated by immersion into boiling deionized water under stirring for 30 min and then dried at 65 °C in vacuum. Calcined and rehydrated solids were used as catalysts. These samples will be referred to as HT_x-caT and HT_x-rh, respectively, where x = 30, 50, 61, 70 or 100, and T is the calcination temperature (°C). Note that as x increases the molar Mg/Al ratio increases as well.

2.2. Catalysts characterization

X-ray diffraction (XRD) patterns of the powdered samples were obtained using a Siemens D5000 diffractometer operating with Cu Kα radiation (λ = 1.5405 Å), at 45 mA, 40 kV, 2θ scanning range 20–80° and scan step size of 0.05°. Raman spectra were obtained in a dispersive Raman microscope Jobin Yvon LabRam HR using green laser (514.5 nm). Thermogravimetric analyses were performed in a Seiko Exstar 6000 thermobalance under oxygen flow and heating rate of 5 °C/min. The N_2 adsorption–desorption isotherms at −196 °C were measured by the static method in an automatic volumetric Micromeritics® ASAP 2000 adsorption analyzer. Prior to the measurements, samples were degassed for 2 h at 80 °C. Specific surface areas (S_{BET}) were calculated using the BET method from the nitrogen adsorption isotherms taking a value of 0.162 nm^2 for the cross-sectional area of the adsorbed N_2 molecule. Specific total pore volumes (V_p) were assessed from the amount of nitrogen adsorbed at a relative pressure of 0.99, assuming that the density of the nitrogen condensed in the pores is equal to that of liquid nitrogen at −196 °C (1.547 g/cm^3).

The basic strength (H_-) and basicity, or basic sites density ($mmol/g_{cat}$), were determined according to the methods based on the colour change of acid indicators and titration with benzoic acid, respectively [13,50]. The value of H_- is approximately given by the pK_a of the acid indicator showing upon adsorption a colour intermediate between those of the acidic and basic forms. The indicators employed in this work (their pK_a values are given in parentheses) were: bromothymol blue (7.2), phenolphthalein (9.3), thimolphthalein (9.9), alizarine yellow (11.0) and indigo carmine (12.2). The determination of H_- was carried out placing about 100 mg of the solid in a test tube, adding about 2 ml of a solution of the indicator in methanol and shaking vigorously. After equilibration, the suspension was examined for colour change. Regarding the measurement of the basicity, suspensions with 50 mg of the solid in 20 ml of methanol containing the indicator were prepared and maintained under vigorous stirring. The suspensions were titrated with solutions 0.0125 or 0.2 M of benzoic acid in methanol depending on the indicator used.

The basic properties of selected solids were also characterized by CO_2-TPD with mass spectrometry detection (TPD–MS) that was carried out in a conventional continuous flow U-shaped quartz reactor working at atmospheric pressure. About 80 mg of the catalyst was placed between two plugs of quartz wool; the temperature was monitored by a thermocouple in contact with the catalyst bed. The desorbed products were analyzed by mass spectrometry, using a Balzers Thermostar mass spectrometer controlled by Balzers Quadstar 422 software. CO_2 desorption profiles were recorded by monitoring the signal corresponding to the molecular ion (m/z = 44) from room temperature to 900 °C at a heating rate of 10 °C/min although no CO_2 was desorbed above 650 °C. Samples were loaded into the reactor immediately after the calcination or rehydration treatment and allowed to equilibrate with a flow of 30 ml/min of pure CO_2 at room temperature. Then helium (30 ml/min) was introduced as carrier gas and after 30 min the temperature programme was run.

2.3. Transesterification reactions

Transesterification reactions were carried out in a Radleys Carousel Tornado IS6 system with capacity for carrying out simultaneously up to 6 catalytic runs. Each reaction was performed in a 100 ml round bottomed flask closed hermetically and with mechanical stirring. The flasks are directly heated by the hotplate where they lean which allows a reaction temperature control

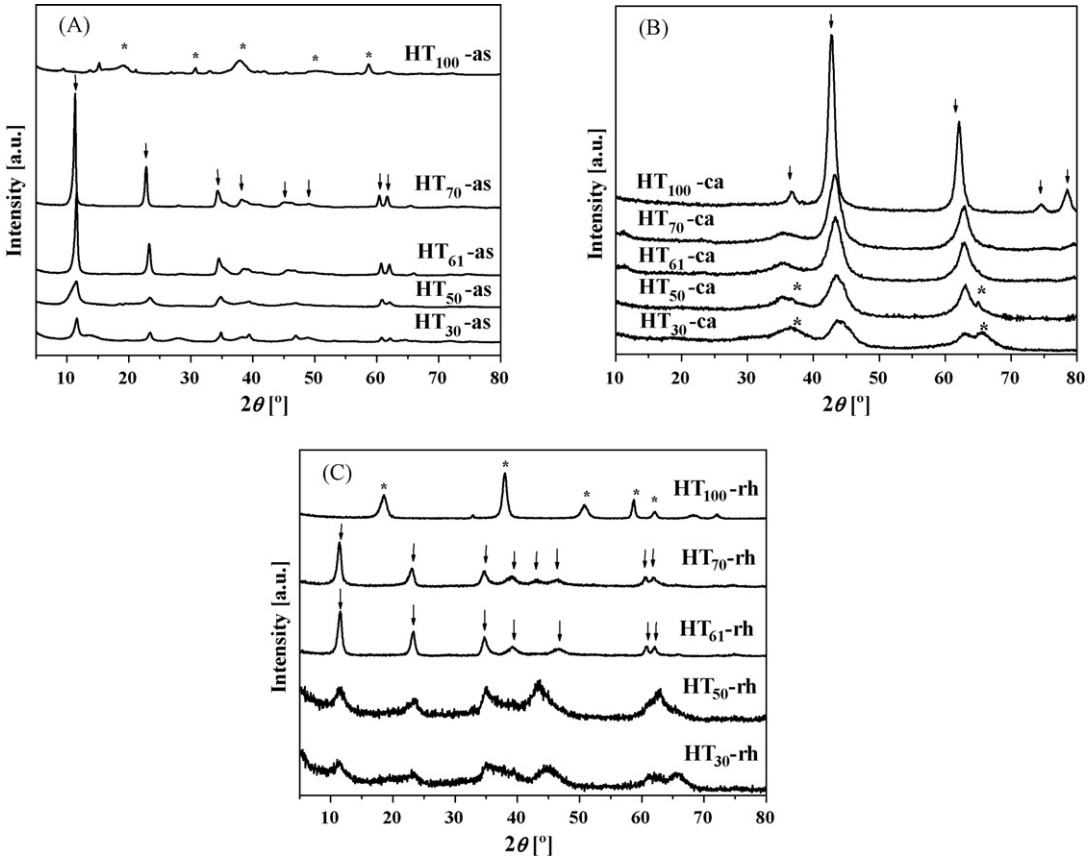

Fig. 1. XRD patterns of the as-received (A, hydrotalcite (↓), $Mg(OH)_2$ (*)), calcined at 500 °C (B, MgO (↓), $MgAl_2O_4$ (*)) and rehydrated (C, hydrotalcite (↓), $Mg(OH)_2$ (*)) samples.

within ±0.5 °C. The lateral neck of the flasks was adapted to fit a type K thermocouple and the inlet and outlet of a recirculation loop made of 1/8 in. teflon tubing and comprising a diaphragm-type metering pump (ProMinent Gugal type G) and a stainless steel three-way ball valve for sampling purposes. Reactions were carried out with HPLC grade methanol (Scharlau) and refined sunflower oil (Urzante, Navarra, Spain, acid value of 0.07 mg KOH/g); a molecular weight of 879.5 g/mol was assumed for the sunflower oil [51]. All the experiments were performed at atmospheric pressure, 60 °C and methanol/oil molar ratio of 12. When using the calcined samples as catalysts, they were weighted and transferred immediately after the thermal treatment into the reaction flask containing hot oil to minimize the interaction with ambient water and CO_2. In the case of the reactions catalyzed by the rehydrated solids, they were also used immediately after the final drying at 65 °C under vacuum. In a typical catalytic run, 30 g of sunflower oil and the required amount of solid catalyst were placed in a round bottomed flask and heated in the Radleys Carousel system under vigorous stirring. When the reaction temperature (60 °C) was attained and stabilized, 13.1 g of methanol (methanol/oil molar ratio = 12) was rapidly added and the recirculation pump switched on. Samples (about 0.5 g) were taken at various intervals through the three-way valve and stored in sealed glass flasks. The reaction was short-stopped by addition of some drops of a glacial acetic acid (Scharlau, HPLC grade) solution (0.6 N) in tetrahydrofuran (THF, Scharlau, HPLC grade) to neutralize the catalysts. Samples were further diluted with about 14 g of additional THF. Once filtered with Acrodisc® syringe filters with 0.2 μm nylon membrane, samples were analyzed by size exclusion chromatography (SEC) with differential refractive index detector at room temperature as described elsewhere [52].

2.4. Catalysts stability

The chemical stability of the catalysts under reaction conditions has been investigated analyzing the possible presence of leached Mg and Al in the reaction mixture. Some of the samples taken from the reaction system to monitor the evolution of the methanolysis reaction were carefully filtered and then introduced in a rotary evaporator at room temperature. After evaporation, the dry fraction was treated with 50 ml of HCl 0.1 N. The resulting solution was analyzed by radial Inductively Coupled Plasma-Atomic Emission Spectroscopy (ICP-AES, Varian MPX) in order to determine the Mg and Al concentration. Leached compounds were referred to the total metal in the sample withdrawn from the reactor assuming that all components in the reactor are perfectly mixed.

3. Results and discussion

3.1. Catalysts characterization

3.1.1. X-ray diffraction and Raman spectroscopy

The XRD patterns of the as-received samples are shown in Fig. 1A. It can be seen that, with the exception of HT_{100}-as, the samples showed the diffraction peaks characteristic of the hydrotalcite structure. The crystallinity increased with the Mg content as it is apparent from the intensification of the diffraction peaks of HT_{70}-as and HT_{61}-as compared to HT_{50}-as and HT_{30}-as. In the case of HT_{100}-as, the XRD data confirmed that this sample mainly consisted of $Mg(OH)_2$. The as-received solids were further characterized by Raman spectroscopy and the corresponding spectra are included in Fig. 2A. Typical bands of hydrotalcites were present [53,54]: Al–O vibration at 360 cm^{-1}, Mg–OH and Al–OH

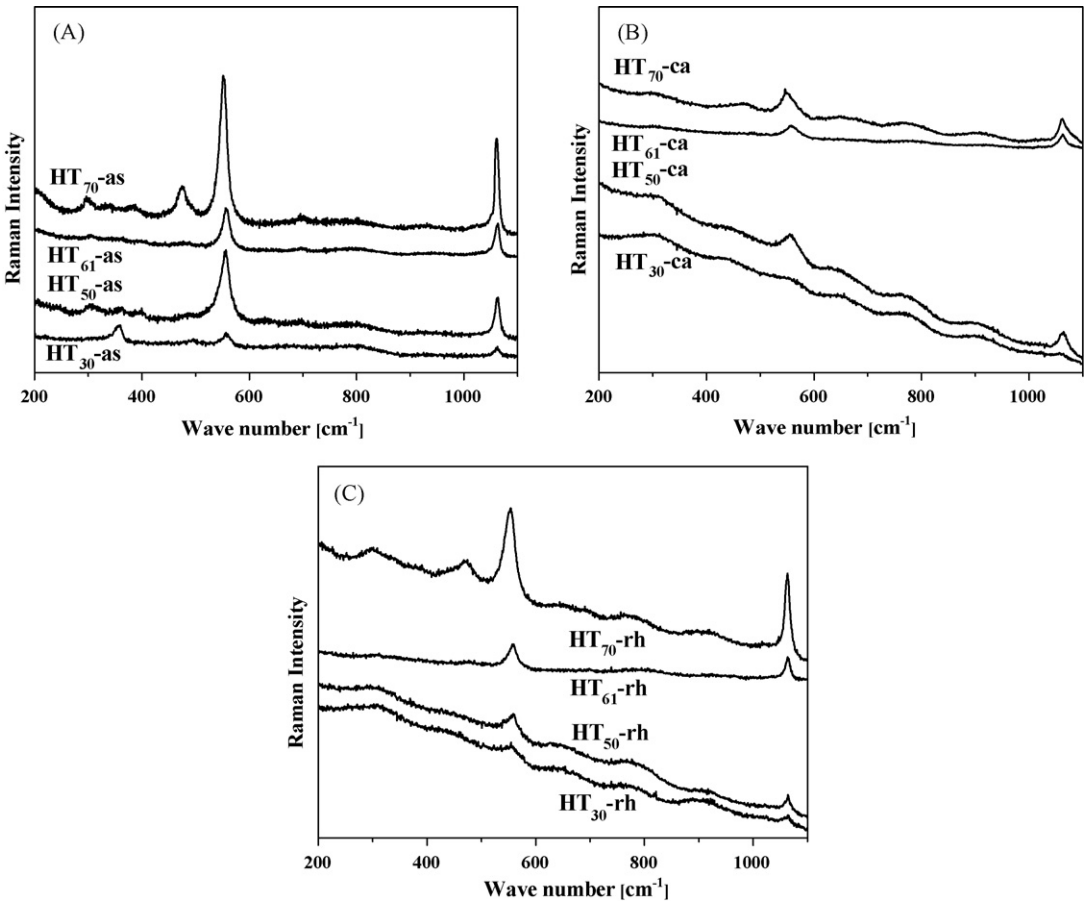

Fig. 2. Raman spectra of as-received (A), calcined at 500 °C (B) and rehydrated (C) samples.

translations at 475 and 553 cm^{-1}, respectively, and a band at 1058 cm^{-1} corresponding to $(Mg,Al)_3$–OH deformation although it could also be related with carbonate associated with the Al_3OH and Mg_3OH units [55]. In the case of HT_{100}-as (spectrum not shown) two bands were perceptible at 276 and 443 cm^{-1} corresponding to hydroxide vibrations of $Mg(OH)_2$ [56].

Upon calcination at 500 °C, the as-received solids underwent decarbonization and dehydration processes that led to the formation of metal oxides. As shown in Fig. 1B, the XRD patterns of the calcined samples with the highest Al contents, HT_{30}-ca500 and HT_{50}-ca500 suggested the presence of amorphous alumina and/or $MgAl_2O_4$. The crystallinity of these solids also increased with the Mg content; HT_{100}-ca500 is a very crystalline MgO. In the Raman spectra of the calcined solids (Fig. 2B) the bands at 475, 553 and 1058 cm^{-1} were very weak, especially for the HT_{30}-ca500 sample. As found by Kloprogge et al. [54] through heating stage Raman microscopy measurements, upon heating and subsequent dehydration these bands decreased in intensity due to changes in the stacking order of the hydroxide. The end of the dehydroxylation process took place at about 400 °C and new bands were observed in the 713–1075 cm^{-1} region indicating the formation of the spinel ($MgAl_2O_4$) [54]. However, decarbonization was incomplete at this stage since bands associated to carbonate species were also perceptible such as the one at 1053 cm^{-1}. López Nieto et al. [57] also

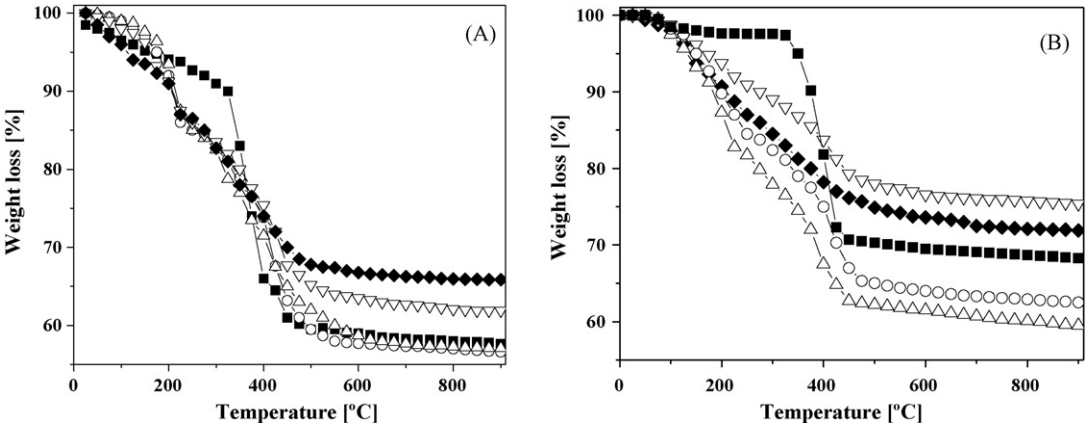

Fig. 3. Thermogravimetric analysis of as-received (A) and rehydrated (B) solids. HT_{100} (■), HT_{70} (○), HT_{61} (△), HT_{50} (▽), HT_{30} (♦).

registered these bands for a hydrotalcite with Mg/Al ratio of 2.77 calcined at 600 °C. On the other hand, the vibration band of carbonate on MgO was detected at 1087 cm^{-1} [55] in the Raman spectrum of HT_{100}-ca500 (not shown).

As concerns the solids rehydrated after calcination, the XRD patterns depicted in Fig. 1C show that samples HT_{61}-rh and HT_{70}-rh recovered their original layered structure which resulted in meixnerite ($Mg_6Al_2(OH)_{18}{\cdot}4H_2O$) formation, a material in which hydroxides are the only compensating anions present in the interlayer space [58–60]. This characteristic is called as retro-topotactical transformation and also known as "memory effect" [48]. On the other hand, whereas HT_{100}-rh recovered the $Mg(OH)_2$ structure HT_{50}-rh and HT_{30}-rh remained as amorphous solids, although the presence of a meixnerite-like phase could be suggested from the XRD patterns. It can be concluded that the Mg/Al ratio has a strong influence on the behaviour of these materials. Indeed, as the Mg/Al ratio increases more ordered calcined or rehydrated materials are obtained. The Raman spectrum of HT_{70}-rh (Fig. 2C) clearly showed the vibration bands at 475 and 552 cm^{-1} characteristic of the hydrotalcite structure. For the rest of rehydrated samples the bands were much weaker. The band at 1061 cm^{-1} corresponding to carbonate species was clearly visible and its presence can be explained by the fact that these samples have been exposed to atmospheric air, thus allowing the adsorption of CO_2 onto Brönsted basic sites as shown by Abelló et al. [61].

3.1.2. Thermogravimetric analyses (TGA)

The TGA profiles of the as-received hydrotalcites are depicted in Fig. 3A. In contrast to HT_{100}-as, the hydrotalcites experienced a first weight loss process until about 250 °C which involved the loss of physically adsorbed water and water in the interlayer space [62] amounting to 15% of the original weight. Between 250 and 500 °C the hydrotalcites lost an additional 20–28% of their weight that can be attributed to structural hydroxide ions in the brucite-like layers and the decomposition of carbonate anions in the interlayer region in accordance with the results reported by Kloprogge et al. [53,54]. HT_{100}-as showed a more gradual weight loss of up to 42% at 500 °C which corresponded to the decomposition of $Mg(OH)_2$ to MgO as well as the loss of adsorbed water and CO_2. The total weight loss increased with the Mg/Al ratio, from about 35–38% for HT_{30}-as and HT_{50}-as to 43% for HT_{61}-as and HT_{70}-as. The differences originated in the 250–500 °C temperature range since up to 250 °C all the solids lost roughly 15% of their weight as mentioned above. This is in accordance with the fact that at high temperatures both the structural hydroxide and interlayer carbonate ions are lost because, due to the different Mg/Al ratio, it can be expected that the proportions of hydrotalcite, brucite and boehmite were also different among these samples. Actually, according to the manufacturer, the content of boehmite in HT_{30}-as was significant which could justify the lower weight loss of this sample due to a lower content of the hydrotalcite phase.

As concerns the rehydrated solids, the weight losses were lower than for their as-received counterparts, as shown in Fig. 3B. The solids with high Mg/Al ratio, HT_{61}-rh and HT_{70}-rh, were the only ones that experienced losses above 35%. In the case of HT_{100}-rh the weight loss of about 30% corresponded to the dehydration of $Mg(OH)_2$ to MgO which is in accordance with the XRD results showing that the brucite structure was restored in the rehydrated sample. The lower weight losses can be readily explained taking into account that rehydration led to two hydroxide anions (34 Da) in the interlayer region per each original carbonate ion (60 Da). On the other hand, the fact that the weight loss increased with the Mg/Al ratio can be related with an easier rehydration of the samples with higher magnesium content. Abelló et al. [47] also found that better reconstructed hydrotalcites showed also higher weight losses in the TGA experiments. The XRD results have evidenced the good crystallinity of HT_{61}-rh, HT_{70}-rh and HT_{100}-rh, whereas HT_{30}-rh and HT_{50}-rh were amorphous (Fig. 1C). These results indicated that the rehydration method used in this study has been particularly effective with the samples having relatively high Mg/Al ratios, allowing a good reconstruction of the hydrotalcite-like (meixnerite) structure.

3.1.3. Nitrogen adsorption

The specific surface areas (S_{BET}) and specific total pore volumes (V_p) of the several samples are compiled in Table 1. As can be seen, there are significant differences among samples. In the case of the as-received hydrotalcites, the solid with the lowest Mg/Al ratio (HT_{30}-as) exhibited the highest surface area and pore volume, whereas the values of these textural parameters decreased considerably for the remaining samples. These results are in accordance with the XRD patterns that showed a clear increase of the crystallinity with the Mg/Al content. Magnesium hydroxide (HT_{100}-as) had specific surface area and pore volumes that were intermediate between those of the high and low surface-area hydrotalcites. Upon calcination the HT_{50}, HT_{61} and HT_{70} hydrotalcites experienced slight to moderate increases of the textural parameters. This is a well-known behaviour of these materials that is attributed to the creation of new porosity as a result of the removal during calcination of carbonate and hydroxide anions from the interlayer space and brucite-like layers, respectively. In our case, the changes affected the mesopores, as judged from the more pronounced hysteresis loops of the adsorption–desorption isotherms and BJH pore size distributions as illustrated in Fig. 4A and B, respectively, for representative samples (HT_{50}-as and HT_{50}-ca500). Some microporosity seems to have been created also

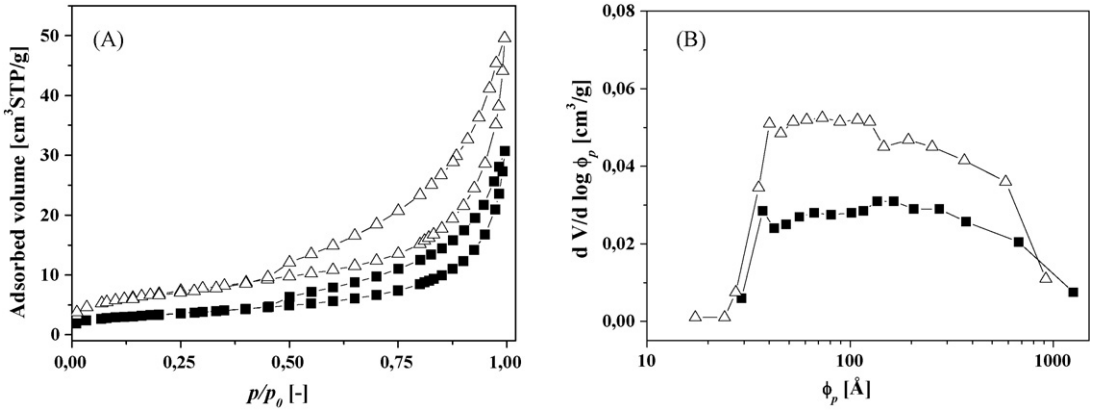

Fig. 4. Nitrogen adsorption isotherms (A) and BJH pore size distributions (B) of the as-received (■) and calcined at 500 °C HT_{50} samples (△).

Table 1
Specific surface areas and total pore volumes of the samples indicated.

Sample	S_{BET} (m^2/g)	V_p (cm^3/g)
HT_{100}		
-as	88	0.23
-ca500	130	0.50
-rh	93	0.28
HT_{70}		
-as	20	0.09
-ca500	26	0.10
-rh	6	0.02
HT_{61}		
-as	49	0.14
-ca500	59	0.16
-rh	51	0.17
HT_{50}		
-as	12	0.03
-ca500	25	0.05
-rh	12	0.02
HT_{30}		
-as	162	0.29
-ca500	167	0.37
-rh	172	0.36

in the calcined samples. Working with a hydrotalcite with Mg/Al ratio of 2, Roelofs et al. [63] found an important increase of the BET surface area (from 88 to 253 m^2/g) upon calcination at 450 °C, as well as the creation of some microporosity.

The reconstruction of the hydrotalcite structure is usually accompanied by the recovery of the original textural properties. In our case, the rehydration of the calcined hydrotalcites gave rise to values of the specific surface area similar to that of the as-received materials with the exception of the sample HT_{70}-rh. This was the solid showing the best reconstruction of the hydrotalcite structure; however, as shown in Fig. 5 there is a clear loss of pore volume in the complete range of pore sizes. Similar results were found by Abelló et al. [47] for well-reconstructed hydrotalcites obtained by rehydration using steam instead of boiling water. In the case of HT_{100}-rh, the reconstruction of the brucite structure was also accompanied by the recovery of the original textural properties.

3.1.4. Basic properties

Basic strength (H_-) of the several samples was determined using different acid–base indicators; the results are compiled in Table 2. Due to the limitations of the methods based on the use of Hammett indicators for heterogeneous (liquid/solid) systems the results included in this table can be considered only in a qualitative way.

The rehydrated hydrotalcites HT_{70}-rh and HT_{61}-rh were the solids exhibiting the strongest basic sites which can be likely

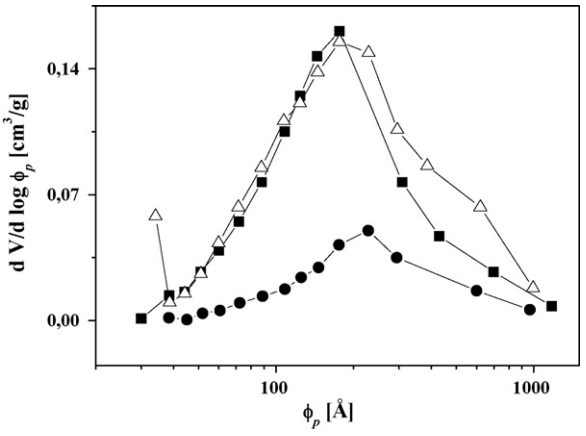

Fig. 5. BJH pore size distributions of the as-received (■), calcined at 500 °C (△) and rehydrated HT_{70} samples (●).

Table 2
Basic properties of the samples indicated.

Sample	Basic strength	Basicity (mmol/$g_{cat.}$)		
		$H_- \geq 7.2$	$H_- \geq 9.3$	$H_- \geq 11$
HT_{100}				
-ca500	$9.9 < H_- < 11.0$	10.0	3.9	0
-rh	$9.3 < H_- < 9.9$	0.9	0	0
HT_{70}				
-ca500	$9.9 < H_- < 11.0$	2.3	1.9	0
-rh	$11.0 < H_- < 12.2$	3.7	2.2	1.1
HT_{61}				
-ca500	$9.3 < H_- < 9.9$	1.3	1.4	0
-rh	$11.0 < H_- < 12.2$	4.7	2.3	0.3
HT_{50}				
-ca500	$9.3 < H_- < 9.9$	1.7	1.5	0
-rh	$9.3 < H_- < 9.9$	0.1	0.1	0
HT_{30}				
-ca500	$9.3 < H_- < 9.9$	2.9	1.4	0
-rh	$9.3 < H_- < 9.9$	1.1	0.4	0

attributed to the presence of hydroxide anions in the interlayer space. Nevertheless, it is usually considered that for rehydrated hydrotalcites, the most active sites seem to be located at the edges and defects of the platelets [61]. In contrast, HT_{50}-rh and HT_{30}-rh showed basic strengths similar to that of their calcined counterparts, having basic sites weaker than those in HT_{70}-rh and HT_{61}-rh. Regarding the basicity, the differences among samples were also clear. For both HT_{70} and HT_{61}, rehydration gave rise to an increased amount of the strongest basic sites. These samples were the only ones having basic sites as strong ($H_- \geq 11.0$) as to change the colour of alizarine yellow. On the other hand, rehydration of HT_{50}-rh and HT_{30}-rh had detrimental consequences on the basicity of these solids. The fact that HT_{50}-rh and HT_{30}-rh were amorphous whereas HT_{70}-rh and HT_{61}-rh exhibited a well-ordered layered structure could contribute to the significant differences between the basic properties of these samples. It can be expected a higher density of active sites in the hydrotalcites showing an ordered layered structure containing the platelets where the most active sites seem to be located. According to Roelofs et al. [64] these are the accessible sites, which amounted only to 5% of the total.

Calcined solids contained significant amounts of sites with $H_- \geq 9.3$. Xie et al. [65] also found a wide distribution of basic sites in calcined Mg–Al hydrotalcites using Hammett indicators, suggesting that several types of basic sites were present in the solids. These centres covered a broad range of H_- values, from 7.2 to 15.0, and were mainly ascribed to Brønsted hydroxyl groups and coordinatively unsaturated oxide anions of the Lewis type. Di Cosimo et al. [66] identified a variety of basic sites on the surface of calcined hydrotalcites, and classified them as of low (hydroxide groups), medium (Mg–O pairs) and high (oxide anions) basic strength. Whereas calcined hydrotalcites exhibited comparable densities of these different types of sites, HT_{100}-ca500, mainly consisting of MgO, was the solid with the highest content of basic centres with H_- values in the 7.2–11 range. These sites are probably associated to oxide anions on the surface; nevertheless, HT_{100} contained 4.2 wt.% Al. It has been reported that the incorporation of small amounts of Al^{3+} cations to MgO generates surface Lewis acid–strong base pair sites. Therefore, it can be considered that both oxide anions and Lewis acid–base pair sites (Mg^{2+}–O^{2-} and Al^{3+}–O^{2-}) were present in the HT_{100}-ca500 solid. Rehydration of this material (HT_{100}-rh) led to $Mg(OH)_2$ formation showing weaker and much less abundant basic sites.

The different natures and properties of the basic sites of the calcined and rehydrated solids are evidenced by the CO_2-TPD–MS results shown in Fig. 6. In the case of the HT_{100}-ca500 and HT_{70}-ca500 samples the TPD profiles were very similar. CO_2 desorbed between 50 and 300–350 °C suggesting the presence of sites with

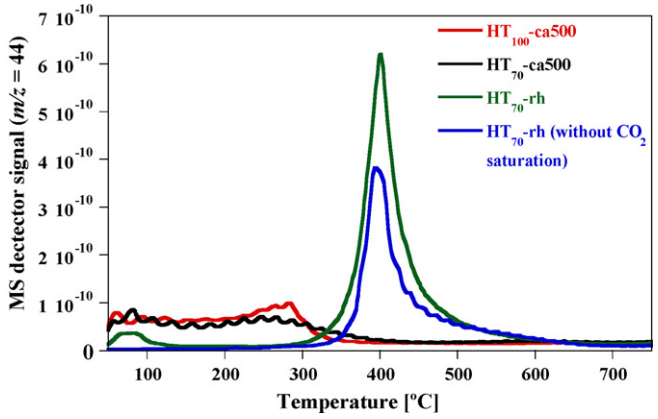

Fig. 6. CO_2-TPD profiles of the samples indicated. Signals correspond to the molecular ion of CO_2 (m/z = 44).

a broad basic strength distribution. The strongest sites of the calcined solids, those corresponding to CO_2 desorption between 250 and 300 °C, were more abundant in the case of HT_{100}-ca500, which is in qualitative accordance with results included in Table 2. As can be seen, the CO_2 desorption profile changed markedly for the rehydrated samples. In the case of the HT_{70}-rh the profile showed a small peak between 50 and 100 °C likely due to physisorbed CO_2 and a second and intense peak with maximum at about 400 °C that evidences the presence of strong sites that should correspond to hydroxide anions in the interlayer space and/or at the edges and defects of the hydrotalcite platelets. A clear desorption peak was also observed when the TPD experiment was carried out without previously saturating the sample with gaseous CO_2. It should be noted that this signal was absent in the profiles of the calcined samples; therefore, it can be interpreted as a proof of the high reactivity of the rehydrated sample surface that became easily carbonated by atmospheric CO_2 as noted by Abelló et al. [61].

3.2. Catalytic performance

3.2.1. Calcined solids

The evolution of the oil conversion with reaction time for the methanolysis of sunflower oil over the solids calcined at 500 °C for 6 h is shown in Fig. 7. Reactions were carried out at 60 °C, methanol/oil molar ratio of 12 and 2 wt.% of catalyst referred to the oil loaded into the reactor. It should be noted that all the as-received

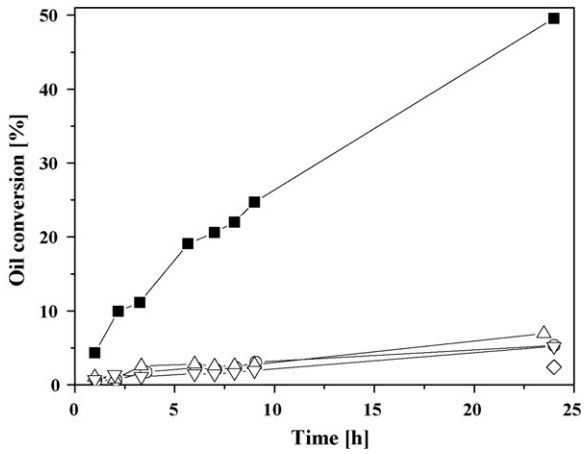

Fig. 7. Evolution of the sunflower oil conversion with reaction time over the catalyst HT_{100} (■), HT_{70} (○), HT_{61} (△), HT_{50} (▽) and HT_{30} (◊) calcined at 500 °C. Reaction conditions: 60 °C, methanol/oil molar ratio of 12 and 2 wt.% of catalyst.

materials were inactive for the synthesis of biodiesel under these experimental conditions. Among the calcined solids, only HT_{100}-ca500 exhibited a significant activity allowing to achieve about 50% oil conversion after 24 h. In contrast, the calcined hydrotalcites yielded a maximum oil conversion of only 5%. Leclercq et al. [40] studied the transesterification with methanol of rapeseed oil with a commercial Mg–Al hydrotalcite (KW 2200, Mg/Al = 2.3) and also established a poor catalytic performance for the as-received material. At the very high methanol/oil ratio of 275, methanol reflux conditions and catalyst concentration of 10 wt.% (referred to the oil) these authors found that, the non-calcined solid yielded 12.5% oil conversion after 22 h that increased up to 34% with the catalyst calcined at 450 °C. As explained by Debecker et al. [48], fresh hydrotalcites usually have poor basic properties due to adsorbed water molecules hindering the access to the basic sites. As a result, these solids are often inactive and have to be activated through thermal decomposition. As discussed in the preceding section, among the calcined solids, HT_{100}-ca500 exhibited the highest content of basic centres with H_- values between 7.2 and 11, and basic sites desorbing CO_2 between 250 and 300 °C that likely consist of oxide anions and Lewis acid–base pair sites. The remaining samples showed very similar basic sites densities (see Table 2). Therefore, the catalytic performance of this series of catalysts correlated well with their basic properties. Xie et al. [65], working with calcined Mg–Al hydrotalcites as catalysts for the methanolysis of soybean oil (methanol/oil = 15, 7.5 wt.% catalyst referred to the oil and methanol reflux conditions) found activities comparable to that of HT_{100}-ca500 in this work; the activity was mainly attributed to coordinatively unsaturated oxide anions acting as Lewis sites. Shumaker et al. [67] also found a direct correlation between the activities of several calcined double layered hydroxides for the methanolysis of glyceryl tributyrate and the presence of medium and strong sites determined by TPD of CO_2. In the case of calcined Zn–Al hydrotalcites, skeletal IR characterization evidenced the formation of labile methoxy groups terminally bonded to Zn^{2+} cations that are considered the species involved in transesterification reactions [68].

In the case of the HT_{100}-ca500 catalyst, the presence of Al^{3+}–O^{2-} acid–base pair sites likely contributes to the relatively good performance of this sample [48]. Indeed, some catalytic runs performed with calcined pure MgO (Sigma–Aldrich, >99%) as catalyst (60 °C, methanol/oil molar ratio of 12 and 2 wt.% catalyst) yielded a maximum oil conversion of 12% after 24 h. This value was higher than the one obtained with the calcined hydrotalcites but clearly lower than the conversion provided by the HT_{100}-ca500 catalyst. This can be explained by the low density of sites with $H_- \geq 7.2$ of MgO (2.9 mmol/g) compared with that of HT_{100}-ca500 (10.0 mmol/g). These results are in accordance with the findings by Di Serio et al. [69] who reported the absence of strong basic sites on the surface of MgO.

It is well-known that the properties of the calcined hydrotalcites are very dependent on the thermal treatments applied [48]. In order to investigate the effects of the calcination conditions, several calcination temperatures (350, 450, 500, 550 and 700 °C) were considered. The evolution of the oil conversion with reaction time for the methanolysis of sunflower oil over the HT_{100} sample calcined at these temperatures is shown in Fig. 8. As can be seen, there is a marked influence of the thermal treatment temperature on the catalytic performance. The oil conversion after 24 h of reaction was 32% for HT_{100}-ca550, about 27% for both HT_{100}-ca350 and HT_{100}-ca450 and 13% for HT_{100}-ca700. These values were clearly lower than the conversion achieved with HT_{100}-ca500; therefore, there is an optimum calcination temperature for this material close to 500 °C. As concerns the remaining samples, it was found that calcination at temperatures other than 500 °C did not improve the catalytic activity. The basic and textural properties of HT_{100}

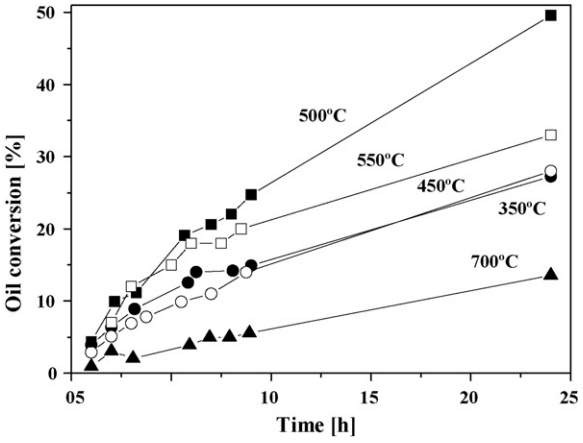

Fig. 8. Evolution of the sunflower oil conversion with reaction time over the catalyst HT_{100} calcined at 350 (●), 450 (○), 500 (■), 550 (□) and 700 °C (▲). Reaction conditions: 60 °C, methanol/oil molar ratio of 12 and 2 wt.% of catalyst.

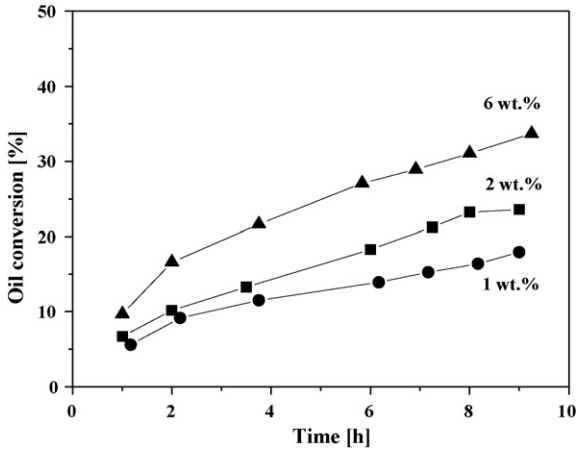

Fig. 9. Evolution of the sunflower oil conversion with reaction time over HT_{100} calcined at 500 °C at catalyst concentration of 1 (●), 2 (■) and 6 wt.% (▲). Other reaction conditions: 60 °C and methanol/oil molar ratio of 12.

calcined at different temperatures are compiled in Table 3. The results in Fig. 8 and Table 3 suggest that the methanolysis activity of the calcined HT_{100} sample was controlled by the presence of basic sites with $H_- \geq 9.3$. Indeed, the basic properties of HT_{100}-ca350 and HT_{100}-ca450 catalysts were similar, like their catalytic performance. On the other hand, the catalysts with the highest density of sites with $H_- \geq 9.3$, HT_{100}-ca500 and HT_{100}-ca550, are the most active ones. Finally, calcination at 700 °C had detrimental effects on the basic properties and, as a result, HT_{100}-ca700 gave the lowest sunflower oil conversions. Xie et al. [65] also found an optimal calcination temperature of 500 °C for a Mg–Al hydrotalcite (Mg/Al = 3.0). Maximum basicity of 3.5 mmol/g was measured after calcination at this temperature using a method similar to that considered in this work, titration with benzoic acid and Hammett indicators. The basicity significantly decreased for calcination temperatures below 400 °C and above 600 °C and the activity for the methanolysis of soybean oil correlated closely with the catalysts basicity. Similar effects of the calcination temperature and the density of basic sites have been reported by several authors [67,70–72].

The effect of the catalyst (HT_{100}-ca500) concentration on the sunflower oil conversion is shown in Fig. 9; reactions were carried out at 60 °C and methanol/oil molar ratio of 12. As expected, the oil conversion increased with the catalyst concentration. After 9 h of reaction the conversions were 17, 23 and 34% for catalyst concentrations of 1, 2 and 6 wt.%, respectively. Due to their intrinsic lower activity compared with the homogeneous catalysts, significantly higher concentrations of the heterogeneous transesterification catalysts are required [30], especially when using low-quality feedstocks such as used frying oil (10–12 wt.%) [73–75] or animal fats (10–20 wt.%) [76]. Xie et al. [65] measured 67% soybean oil methanolysis conversion after 9 h of reaction at methanol reflux conditions, methanol/oil molar ratio of 15 and 7.5 wt.% of a Mg–Al hydrotalcite (Mg/Al = 3) calcined at 500 °C. Very good results have been reported with a similar hydrotalcite by Zeng et al. [72,77] who obtained 90–94% rapeseed oil conversion after 3–4 h of reaction at 65 °C with methanol/oil molar ratio of 6 and 1.5–2 wt.% of catalyst.

Biodiesel standards [78] establish strict limits to the contents of monoglycerides and diglycerides in the final product so it is interesting to study the evolution of these intermediate compounds as shown in Fig. 10 for the HT_{100}-ca500 catalyst at 60 °C, methanol/oil molar ratio of 12 and 2 wt.% of catalyst. The monoglyceride and diglyceride yields increased slightly with reaction time, achieving 4 and 6%, respectively, after 24 h. This led to selectivity values to monoglycerides, diglycerides and biodiesel of 9, 13 and 78%, respectively. Therefore, the presence of intermediate transesterification products was significant as is also typical of methanolysis with homogeneous catalysts at intermediate levels of oil conversion, as found by Arzamendi et al. [22,30,52]. These values are also close to the ones obtained by the authors for the methanolysis of sunflower oil over NaOH/γ-alumina [30] and NaOH/silica [34]. Much higher selectivities for monoglycerides and diglycerides, up to 40 and 30%, respectively, have been measured over CaO and $Ca(OH)_2$ [22].

Table 3
Basic and textural properties of the HT_{100} sample calcined at the temperatures indicated.

Sample	S_{BET} (m^2/g)	V_p (cm^3/g)	Basicity (mmol/$g_{cat.}$)	
			$H_- \geq 7.2$	$H_- \geq 9.3$
HT_{100}				
-ca350	208	0.51	10.9	3.0
-ca450	142	0.48	10.4	3.0
-ca500	130	0.50	10.0	3.9
-ca550	102	0.50	8.1	3.3
-ca700	56	0.44	0.8	0.4

3.2.2. Rehydrated hydrotalcites

The evolution of the oil conversion with reaction time for the methanolysis of sunflower oil over the rehydrated solids is shown

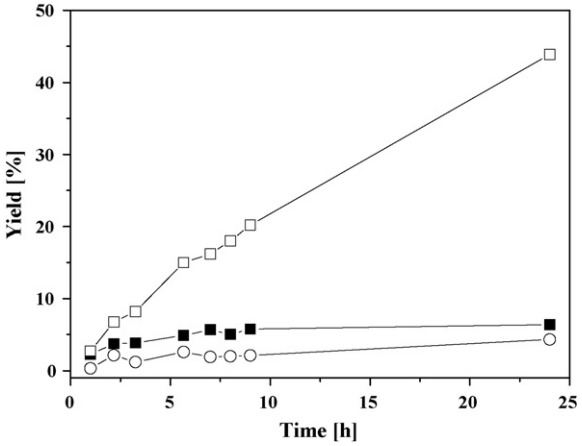

Fig. 10. Evolution with reaction time of the yields to monoglycerides (○), diglycerides (■) and biodiesel (□) over the HT_{100} catalyst calcined at 500 °C. Reaction conditions: 60 °C, methanol/oil molar ratio of 12 and 2 wt.% of catalyst.

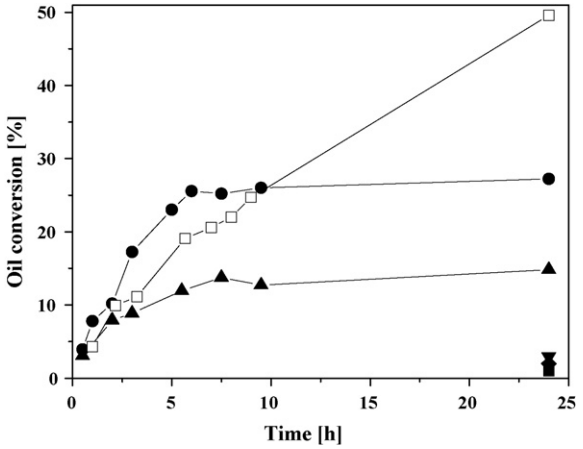

Fig. 11. Evolution of the sunflower oil conversion with reaction time over the catalyst HT_{100}-ca500 (□), HT_{70}-rh (●), HT_{61}-rh (▲), HT_{50}-rh (▼), HT_{30}-rh (♦) and HT_{100}-rh (■) catalysts. Reaction conditions: 60 °C, methanol/oil molar ratio of 12 and 2 wt.% of catalyst.

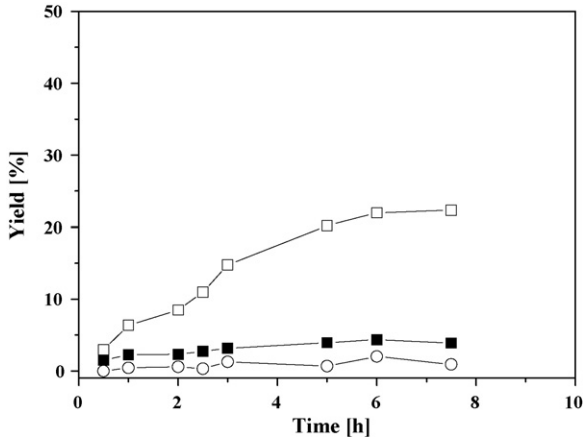

Fig. 12. Evolution with reaction time of the yields to monoglycerides (○), diglycerides (■) and biodiesel (□) over the HT_{70}-rh catalyst calcined at 500 °C. Reaction conditions: 60 °C, methanol/oil molar ratio of 12 and 2 wt.% of catalyst.

in Fig. 11, where the performance of the HT_{100}-ca500 catalyst has been included for comparison. Reactions were carried out at 60 °C, methanol/oil molar ratio of 12 and 2 wt.% of catalyst. The most outstanding result is that both HT_{61}-rh and HT_{70}-rh exhibited a significantly improved activity compared with their calcined counterparts. The oil conversions after 24 h of reaction were 15 and 27% over HT_{61}-rh and HT_{70}-rh, respectively. In contrast, HT_{100}-rh became almost inactive, like HT_{30}-rh and HT_{50}-rh. As for the calcined materials, these results can be correlated with the basic properties of the samples (see Table 2 and Fig. 6). Indeed, the increased activity of HT_{61}-rh and HT_{70}-rh can be attributed to the increase of the density of basic sites showing $H_- \geq 9.3$, and even to the creation of new sites with $H_- \geq 11$ desorbing CO_2 at temperatures as high as 400–450 °C. On the other hand, rehydration had a strong detrimental effect on the basic properties of the remaining solids, especially HT_{100}-rh. As discussed in Section 3.1.4, the fact that HT_{70}-rh and HT_{61}-rh exhibited well-ordered layered structures likely contributed to the improved basic properties associated to strong hydroxide anions in the interlayer space and at the edges and defects of the hydrotalcite platelets. In the case of HT_{100}, rehydration led to $Mg(OH)_2$ formation showing few and weak basic sites thus resulting in very poor catalytic performance. As indicated by Xi and Davis [62], $Mg(OH)_2$ has the brucite layered structure but without the Brønsted basic sites associated with rehydrated hydrotalcites. A similar decrease of sunflower oil methanolysis activity of $Ca(OH)_2$ compared with CaO has been reported previously [22]. Xi and Davis [62,79] studied the transesterification with methanol of tributyrin over synthesized Mg–Al hydrotalcites. It was found that the solids reconstructed after rehydration were much more active than the mixed oxides obtained upon calcination. The authors concluded that the charge-compensating hydroxide anions act as Brønsted sites active for the methanolysis reaction whereas the hydroxide anions in the brucite-like layers are considered to have negligible catalytic activity.

The evolution of the yields to the several transesterification products with reaction time for the HT_{70}-rh catalyst is shown in Fig. 12. After 7.5 h of reaction the monoglycerides, diglycerides and biodiesel yields were about 1.5, 4 and 22%, respectively, and the selectivities 6.8, 18 and 75.2%. This indicates that the rehydrated hydrotalcite was slightly more selective than HT_{100}-ca500 because at the same level of oil conversion the calcined sample gave monoglycerides, diglycerides and biodiesel selectivities of 9, 25 and 66%, respectively.

The mechanistic aspects of the biodiesel synthesis with solid catalysts have been reviewed by Di Serio et al. [10] and Lotero et al. [80,81]. Methanolysis of triglycerides can be catalyzed by basic, both Brønsted and Lewis sites, as well as Lewis acids, whereas Brønsted acids are more active for the synthesis of biodiesel through the esterification route [82,83]. Regarding the use of solid bases, the formation of methoxide species is a key step of the reaction. Once formed this nucleophilic species attacks a carbonyl carbon atom of an ester molecule to form a tetrahedral intermediate. When using Brønsted base catalysts such as modified zeolites or ETS-10 and ETS-4 a homogeneous-like mechanism has been claimed in which the solid acts as a conventional homogeneous Brønsted base (e.g. NaOH or KOH) and a free methoxide species seems to be involved in the reaction [80]. In the case of basic Lewis catalysts such as MgO or CaO, an Eley–Rideal mechanism is usually considered by which an adsorbed methoxide is the active species that attacks the carbonyl carbon atom of an ester molecule in the liquid phase [10]. As discussed above, the presence of strong Brønsted sites seems to be the main feature of the well rehydrated HT_{70}-rh and HT_{61}-rh samples whereas for the calcined materials, specially HT_{100}-ca500, weaker Lewis sites (coordinatively unsaturated oxide anions and Al^{3+}–O^{2-} acid–base pairs) were predominant. The differences in catalytic performance among these solids could be mainly ascribed to the different natures and reactivity of their active sites with respect to the activation of the methanol molecule. In this regard, two types of methoxy species were identified by Montanari et al. [68] upon methanol adsorption on oxides obtained from Zn–Al hydrotalcite precursors. These species showed different stability with respect to desorption, and the most labile was considered likely responsible for the catalyst activity for methanolysis reactions. In our case, a higher reactivity of the free methoxide species generated by Brønsted sites could explain the better selectivity to biodiesel of the rehydrated hydrotalcites.

Chemical stability of the heterogeneous methanolysis catalysts is a key issue since it can condition the catalyst reutilization feasibility as well as the biodiesel purification needs. Chemical analysis of the reaction mixture after use of the HT_{61}-rh and HT_{70}-rh solids showed that no Mg or Al leaching took place. However, it is clear from the evolution of the oil conversion curves shown in Fig. 11 that the rehydrated solids became inactive after about 8 h of reaction. Once recovered after this time, thoroughly washed with THF and calcined and rehydrated again, these samples continued being almost inactive which indicates that they resulted irreversibly deactivated. In contrast, after using and recovering the HT_{100}-ca500

catalyst and treating the solid as described above, the recycled catalyst gave 68% of the original sunflower oil conversion thus showing a partial loss of activity. Liu et al. [76] found that calcined Mg–Al hydrotalcites deactivated by strong adsorption of triglycerides on the catalyst surface. This was shown through experiments precontacting the catalysts with methanol or the oil and comparing the effects of using a vegetable oil or triacetin as triglyceride source. Therefore, it seems reasonable to attribute the activity loss of HT_{100}-ca500 to triglyceride adsorption. Anyway, it can be concluded that the rehydrated samples were more unstable than the calcined HT_{100} solid. Xi and Davis [62] also found that the catalysts containing the most adsorbed water (the rehydrated samples) deactivated faster. This was attributed to the hydrolysis of the methyl esters leading to butyric acid formation that poisoned the basic sites on the catalyst. In our case, it should be noted that HT_{61}-rh and HT_{70}-rh contained above 35 wt.% of water (see Fig. 3B) so it can be expected that the adsorption properties of these solids were greatly influenced by the hydrophilic character of their surface. In this regard, as the methanolysis reaction progressed and the concentration of glycerol increased it is likely that the amount of this polar product adsorbed on the hydrotalcites increases as well which could contribute to the activity loss as noted by Corma et al. [60]. As mentioned above, another possible way of catalyst deactivation is the neutralization of the Brønsted basic sites through reaction with the organic acids resulting from the hydrolysis of the methyl esters. In this work, free fatty acids have not been detected among the reaction products. On the other hand, the rate of the hydrolysis of methyl esters markedly decreases as its acyl chain length increases [84]; therefore, it is reasonable to expect a lower influence of the hydrolysis in our case than in the methanolysis of tributyrin [62]. Nevertheless, the possibility of deactivation caused by hydrolysis reactions cannot be ruled out because the strong adsorption of the fatty acids on the catalysts would make their detection difficult among the reaction products.

4. Summary and conclusions

A series of commercial Mg–Al hydrotalcites (PURAL® MG) have been investigated as precursors of transesterification catalysts for the synthesis of biodiesel from sunflower oil and methanol. In general, the catalytic activity exhibited by the solids included in this study is modest compared with the results reported in the literature for hydrotalcites synthesized at the laboratory, although the relatively low heterogeneous catalyst concentrations (1–6 wt.%) employed in this work should be taken into account. This performance is presumably related to the relatively high Al content of the commercial solids that resulted in low Mg/Al molar ratios in the 0.5–2.3 range.

Physicochemical characterization by XRD, TGA, Raman spectroscopy and nitrogen adsorption allowed to identify the most characteristic features of this type of materials. Regarding the basic properties, the basic strength (H_-) and the density of basic sites were determined by titration with benzoic acid and Hammett indicators; CO_2-TPD–MS of selected samples was carried out as well. A general accordance between the basic properties of the catalysts and their activity for sunflower oil methanolysis has been found. All the as-received materials showed no significant activity so calcination at several temperatures (350–700 °C) and rehydration in boiling water were adopted as activation treatments. Among the calcined solids, only a sample mainly consisting of MgO but containing some Al (4.2 wt.%) was significantly active, achieving 50% oil conversion after 24 h at 60 °C, methanol/oil molar ratio of 12 and 2 wt.% of catalyst referred to the oil. This was the solid exhibiting the highest density of basic sites. Its activity can be attributed to Lewis-type sites as coordinatively unsaturated oxide anions and Al^{3+}–O^{2-} acid–base pairs. Calcination at 500 °C resulted in the best catalytic performance due to a maximum density of sites with $H_- > 9.3$. Rehydration of this solid led to $Mg(OH)_2$ that was inactive indicating that hydroxide anions in the brucite layers are not strong enough for methoxide ion formation. In contrast, the rehydrated hydrotalcites with the highest Mg/Al molar ratios (1.9 and 2.3) showed a significantly improved activity compared with their calcined counterparts. These solids recovered a well-ordered layered structure with hydroxides instead of carbonates as charge-compensating anions in the interlayer space showing basic sites with $H_- > 11$. In this case, the activity can be attributed to Brønsted-type hydroxide anions in specific points of the hydrotalcite platelets. The different natures of the active sites resulted also in selectivity differences. Indeed, at intermediate oil conversion levels, MgO showed more selectivity to monoglycerides (9%) and diglycerides (25%) whereas reconstructed hydrotalcites were more selective (75%) to biodiesel formation. It has been verified that no Mg or Al leaching took place; however, the rehydrated samples deactivated significantly. In the case of MgO, after washing and calcination, the recycled catalyst gave 68% of the original oil conversion.

Acknowledgements

Financial support by the Spanish Ministry of Science and Innovation (TRACE: TRA2009_0265_02, ENE2009-14522-C05-01 and ENE2009-14522-C05-03) is gratefully acknowledged. This work has been co-financed by FEDER funds from European Union. L.F. Bobadilla expresses his gratitude to the Junta de Andalucía for the scholarship granted associated to project POG-TEP01965. W.Y. Hernández thanks the AlBan program for the fellowship awarded (E06D101739CO).

References

[1] Directive 2009/28/EC of the European Parliament and of the Council of 23 April 2009 on the promotion of the use of energy from renewable sources, Off. J. Eur. Union L140 (2009) 16–62.
[2] H. Kim, S. Kim, B.E. Dale, Environ. Sci. Technol. 43 (2009) 961.
[3] S. Pinzi, I.L. Garcia, F.J. Lopez-Gimenez, M.D. Luque de Castro, G. Dorado, M.P. Dorado, Energy Fuels 23 (2009) 2325.
[4] J. Janaun, N. Ellis, Renew. Sust. Energy Rev. 14 (2010) 1312.
[5] Y. Lechón, H. Cabal, C. de la Rúa, N. Caldés, M. Santamaría, R. Sáez, Biomass Bioenergy 33 (2009) 920.
[6] EUROBSERV'ER, Biofuels Barometer. (July) (2009) 54–77.
[7] G. Busca, Ind. Eng. Chem. Res. 48 (2009) 6486.
[8] A.P. Vyas, J.L. Verma, N. Subrahmanyam, Fuel 89 (2010) 1.
[9] G. Knothe, Prog. Energy Combust. Sci. 36 (2010) 364.
[10] M. Di Serio, R. Tesser, L. Pengmei, E. Santacesaria, Energy Fuels 22 (2008) 207.
[11] M. Zabeti, W.M.A.W. Daud, M.K. Aroua, Fuel Process. Technol. 90 (2009) 770.
[12] Z. Helwami, M.R. Othman, N. Aziz, W.J.N. Fernando, J. Kim, Fuel Process. Technol. 90 (2009) 1502.
[13] G. Busca, Chem. Rev. 110 (2010) 2217.
[14] S. Gryglewicz, Bioresour. Technol. 70 (1999) 249.
[15] S. Gryglewicz, Appl. Catal. A: Gen. 192 (2000) 23.
[16] G.J. Suppes, K. Bockwinkel, S. Lucas, J.B. Botts, M.H. Mason, J.A. Heppert, J. Am. Oil Chem. Soc. 78 (2001) 139.
[17] C. Reddy, V. Reddy, R. Oshel, J.G. Verkade, Energy Fuels 20 (2006) 1310.
[18] L. Wang, H. He, Z. Xie, J. Yang, S. Zhu, Fuel Process. Technol. 88 (2007) 477.
[19] M. López Granados, M.D. Zafra Poves, D. Martín Alonso, R. Mariscal, F. Cabello Galisteo, R. Moreno-Tost, J. Santamaría, J.L.G. Fierro, Appl. Catal. B: Environ. 73 (2007) 317.
[20] M. Kouzu, T. Kasuno, M. Tajika, S. Yamanaka, J. Hidaka, Appl. Catal. A: Gen. 334 (2008) 357.
[21] I.N. Martyanov, A. Sayari, Appl. Catal. A: Gen. 339 (2008) 45.
[22] G. Arzamendi, E. Arguiñarena, I. Campo, S. Zabala, L.M. Gandía, Catal. Today 133–135 (2008) 305.
[23] Y. Wang, F. Zhang, S. Xu, L. Yang, D. Li, D.G. Evans, X. Duan, Chem. Eng. Sci. 63 (2008) 4306.
[24] J.M. Rubio-Caballero, J. Santamaría-González, J. Mérida-Robles, R. Moreno-Tost, A. Jiménez-López, P. Maireles-Torres, Appl. Catal. B: Environ. 91 (2009) 339.
[25] O.S. Stamenković, V.B. Veljković, Z.B. Todorović, M.L. Lazić, I.B. Banković-Ilić, D.U. Skala, Bioresour. Technol. 101 (2010) 4423.
[26] Z. Wen, X. Yu, S.-T. Tu, J. Yan, E. Dahlquist, Appl. Energy 87 (2010) 743.
[27] T. Ebiura, T. Echizen, A. Ishikawa, K. Murai, T. Baba, Appl. Catal. A: Gen. 283 (2005) 111.

[28] W. Xie, H. Peng, L. Chen, Appl. Catal. A: Gen. 300 (2006) 67.
[29] W. Xie, H. Li, J. Mol. Catal. A: Chem. 255 (2006) 1.
[30] G. Arzamendi, I. Campo, E. Arguiñarena, M. Sánchez, M. Montes, L.M. Gandía, Chem. Eng. J. 134 (2007) 123.
[31] I. Lukić, J. Krstić, D. Jovanović, D. Skala, Bioresour. Technol. 100 (2009) 4690.
[32] M. Verziu, M. Florea, S. Simon, V. Simon, P. Filip, V.L. Parvulescu, C. Hardacre, J. Catal. 263 (2009) 56.
[33] M. Zabeti, W.M.A.W. Daud, M.K. Aroua, Fuel Process. Technol. 91 (2010) 243.
[34] G. Arzamendi, I. Campo, E. Arguiñarena, M. Sánchez, M. Montes, L.M. Gandía, J. Chem. Technol. Biotechnol. 83 (2008) 862.
[35] M.C.G. Albuquerque, I. Jiménez-Urbistondo, J. Santamaría-González, J.M. Mérida-Robles, R. Moreno-Tost, E. Rodríguez-Castellón, A. Jiménez-López, D.C.S. Azevedo, C.L. Cavalcante Jr., P. Maireles-Torres, Appl. Catal. A: Gen. 334 (2008) 35.
[36] Y. Du, S. Liu, Y. Ji, Y. Zhang, S. Wei, F. Liu, F.-S. Xiao, Catal. Lett. 124 (2008) 133.
[37] P. De Filippis, C. Borgianni, M. Paolucci, Energy Fuels 19 (2005) 2225.
[38] M. Di Serio, M. Cozzolino, R. Tesser, P. Patrono, F. Pinzari, B. Bonelli, E. Santacesaria, Appl. Catal. A: Gen. 320 (2007) 1.
[39] G. Guan, K. Kusakabe, S. Yamasaki, Fuel Process. Technol. 90 (2009) 520.
[40] E. Leclercq, A. Finiels, C. Moreau, J. Am. Oil Chem. Soc. 78 (2001) 1161.
[41] G.J. Suppes, M.A. Dasari, E.J. Doskocil, P.J. Mandiky, M.J. Goff, Appl. Catal. A: Gen. 257 (2004) 213.
[42] A. Brito, M.E. Borges, N. Otero, Energy Fuels 21 (2007) 3280.
[43] M.J. Ramos, A. Casas, L. Rodríguez, R. Romero, A. Pérez, Appl. Catal. A: Gen. 346 (2008) 79.
[44] D.E. López, J.G. Goodwin Jr., D.A. Bruce, E. Lotero, Appl. Catal. A: Gen. 295 (2005) 97.
[45] F. Cavani, F. Trifirò, A. Vaccari, Catal. Today 11 (1991) 173.
[46] V. Rives, Mater. Chem. Phys. 75 (2002) 19.
[47] S. Abelló, F. Medina, D. Tichit, J. Pérez-Ramírez, J.C. Groen, J.E. Sueiras, P. Salagre, Y. Cesteros, Chem. Eur. J. 11 (2005) 728.
[48] D.P. Debecker, E.M. Gaigneaux, G. Busca, Chem. Eur. J. 15 (2009) 3920.
[49] B.F. Sels, D.E. De Vos, P.A. Jacobs, Catal. Rev. 43 (2001) 443.
[50] K. Tanabe, M. Misono, Y. Ono, H. Hattori, Studies in Surface Science and Catalysis, vol. 51, Elsevier, Kodansha, Tokyo, 1989, pp. 14–25.
[51] B. Freedman, E.H. Pryde, T.L. Mounts, J. Am. Oil Chem. Soc. 61 (1984) 1638.
[52] G. Arzamendi, E. Arguiñarena, I. Campo, L.M. Gandía, Chem. Eng. J. 122 (2006) 31.
[53] J.T. Kloprogge, R.L. Frost, Appl. Catal. A: Gen. 184 (1999) 61.
[54] J.T. Kloprogge, L. Hickey, R.L. Frost, Appl. Clay Sci. 18 (2001) 37.
[55] T.E. Johnson, W. Martens, R.L. Frost, Z. Ding, J.T. Kloprogge, J. Raman Spectrosc. 33 (2002) 604.
[56] J.T. Kloprogge, L. Hickey, R.L. Frost, J. Raman Spectrosc. 35 (2004) 967.
[57] J.M. López Nieto, A. Dejoz, M.I. Vazquez, Appl. Catal. A: Gen. 132 (1995) 41.
[58] K.K. Rao, M. Gravelle, J. Sanchez Valente, F. Figueras, J. Catal. 173 (1998) 115.
[59] J. Rocha, M. del Arco, V. Rives, M.A. Ulibarri, J. Mater. Chem. 99 (1999) 2499.
[60] A. Corma, S.B. Abd Hamid, S. Iborra, A. Velty, J. Catal. 234 (2005) 340.
[61] S. Abelló, D. Vijaya-Shankar, J. Pérez-Ramírez, Appl. Catal. A: Gen. 342 (2008) 119.
[62] Y. Xi, R.J. Davis, J. Catal. 254 (2008) 190.
[63] J.C.A.A. Roelofs, A.J. van Dillen, K.P. de Jong, Catal. Today 60 (2000) 297.
[64] J.C.A.A. Roelofs, D.J. Lensveld, A.J. van Dillen, K.P. de Jong, J. Catal. 203 (2000) 184.
[65] W. Xie, H. Peng, L. Chen, J. Mol. Catal. A: Chem. 246 (2006) 24.
[66] J.I. Di Cosimo, V.K. Díez, M. Xu, E. Iglesia, C.R. Apesteguía, J. Catal. 178 (1998) 499.
[67] J.L. Shumaker, C. Crofcheck, S.A. Tackett, E. Santillan-Jimenez, T. Morgan, Y. Ji, M. Crocker, T.J. Toops, Appl. Catal. B: Environ. 82 (2008) 120.
[68] T. Montanari, M. Sisani, M. Nocchetti, R. Vivani, M.C. Herrera Delgado, G. Ramis, G. Busca, U. Costantino, Catal. Today 152 (2010) 104.
[69] M. Di Serio, M. Ledda, M. Cozzolino, G. Minutillo, R. Tesser, E. Santacesaria, Ind. Eng. Chem. Res. 45 (2006) 3009.
[70] J.L. Shumaker, C. Crofcheck, S.A. Tackett, E. Santillan-Jimenez, M. Crocker, Catal. Lett. 115 (2007) 56.
[71] W.M. Antunes, C. de Oliveira Veloso, C.A. Henriques, Catal. Today 133–135 (2008) 548.
[72] H. Zeng, Z. Feng, X. Deng, Y. Li, Fuel 87 (2008) 3071.
[73] A. Brito, M.E. Borges, M. Garín, A. Hernández, Energy Fuels 23 (2009) 2952.
[74] R. Sree, N.S. Babu, P.S. Sai Prasad, N. Lingaiah, Fuel Process. Technol. 90 (2009) 152.
[75] K.G. Georgogianni, A.P. Katsoulidis, P.J. Pomonis, M.G. Kontominas, Fuel Process. Technol. 90 (2009) 671.
[76] Y. Liu, E. Lotero, J.G. Goodwin Jr., X. Mo, Appl. Catal. A: Gen. 331 (2007) 138.
[77] H.-Y. Zeng, X. Deng, Y.-J. Wang, K.-B. Liao, AIChE J. 55 (2009) 1229.
[78] G. Knothe, J. Krahl, J. Van Gerpen (Eds.), The Biodiesel Handbook, AOCS Press, Champaign, IL, 2005, pp. 287–294.
[79] Y. Xi, R.J. Davis, J. Catal. 268 (2009) 307.
[80] E. Lotero, J.G. Goodwin Jr., D.A. Bruce, K. Suwannakarn, Y. Liu, D.E. López, in: J.J. Spivey, K.M. Dooley (Eds.), The Catalysis of Biodiesel Synthesis, Catalysis, vol. 19, The Royal Society of Chemistry, Cambridge, 2006, p. 41.
[81] E. Lotero, Y. Liu, D.E. Lopez, K. Suwannakarn, D.A. Bruce, J.G. Goodwin Jr., Ind. Eng. Chem. Res. 44 (2005) 5353.
[82] K. Suwannakarn, E. Lotero, K. Ngaosuwan, J.G. Goodwin Jr., Ind. Eng. Chem. Res. 48 (2009) 2810.
[83] K. Ngaosuwan, E. Lotero, K. Suwannakarn, J.G. Goodwin Jr., P. Praserthdam, Ind. Eng. Chem. Res. 48 (2009) 4757.
[84] P. Khuwijitjaru, T. Fujii, S. Adachi, Y. Kimura, R. Matsuno, Chem. Eng. J. 99 (2004) 1.